

3D printed diffractive terahertz lenses

WALTER D. FURLAN,^{1,*} VICENTE FERRANDO,^{1,2} JUAN A. MONSORIU,² PRZEMYSŁAW ZAGRAJEK,³ ELŻBIETA CZERWIŃSKA,³ AND MIECZYŚLAW SZUSTAKOWSKI³

¹Departamento de Óptica y Optometría y Ciencias de la Visión, Universitat de València, 46100 Burjassot, Spain

²Centro de Tecnologías Físicas, Universitat Politècnica de València, 46022 Valencia, Spain

³Institute of Optoelectronics, Military University of Technology, Warsaw, Poland

*Corresponding author: walter.furlan@uv.es

Received 11 January 2016; revised 17 February 2016; accepted 6 March 2016; posted 7 March 2016 (Doc. ID 257061); published 6 April 2016

A 3D printer was used to realize custom-made diffractive THz lenses. After testing several materials, phase binary lenses with periodic and aperiodic radial profiles were designed and constructed in polyamide material to work at 0.625 THz. The nonconventional focusing properties of such lenses were assessed by computing and measuring their axial point spread function (PSF). Our results demonstrate that inexpensive 3D printed THz diffractive lenses can be reliably used in focusing and imaging THz systems. Diffractive THz lenses with unprecedented features, such as extended depth of focus or bifocalization, have been demonstrated. © 2016 Optical Society of America

OCIS codes: (110.3000) Image quality assessment; (050.1380) Binary optics; (050.1965) Diffractive lenses; (050.1970) Diffractive optics; (110.6795) Terahertz imaging; (220.4610) Optical fabrication.

<http://dx.doi.org/10.1364/OL.41.001748>

Many applications of THz radiation such as THz imaging or THz spectroscopy require passive devices for guiding and manipulating this type of radiation, including filters [1], waveguides [2], waveplates [3], and lenses [4,5]. Several polymers with low absorbance and dispersion [6] are used to obtain THz lenses and, consequently, the variety of commercially available THz lenses is increasing. However, in many cases custom-made THz lenses with a special design are required. Individual refractive THz lenses are mainly manufactured from bulk polymers by milling, turning, or compression molding of polymer powders [5]. In particular, for geometrically complex lenses, this requires high effort and sometimes results in an unwanted waste of material.

In THz setups, beam shaping optical elements are very important in almost every application. Mirrors and lenses should allow improved sensitivity of detection, what is crucial in this range of the electromagnetic radiation, where there is a lack of high-power sources and sensitive detectors. Therefore, as happens in the visible range, THz technology could benefit from novel diffractive structures with unique properties designed for special applications. In fact, some diffractive THz optical elements have been proposed [7–10]; their assessments indicate that the performance of diffractive THz lenses is comparable,

or even better, than that obtained with their refractive homologous. Additionally, diffractive lenses can be fabricated with high numerical aperture [11] and allow for linear and compact setups. However, customized diffractive lenses made by conventional techniques such as reactive ion etching [12] or lathe turning [13] are not widely available because their construction consists of several steps and requires specialized equipment. In this regard, Komlenok *et al.* [14] demonstrated the possibility of fabricating a silicon multilevel THz diffractive optical element, constructed by means of laser ablation process.

Very recently, 3D printing technology has begun to be employed to construct spherical [15], aspherical [16], and hyperbolic lenses [17] for THz and sub-THz radiation ranges. In an effort to provide rapid and low-cost solutions of complex THz lenses in this Letter, we propose the use of 3D printing technology for constructing nonconventional fractal [18] and Fibonacci [19], and THz binary diffractive lenses. The performance of these prototypes was numerically evaluated and experimentally tested.

Several 3D printing materials, including nylon polyamide (PA6) and acrylonitrile-butadiene-styrene (ABS) with two different densities, were tested. In particular, we measured their absorption coefficient and refractive index in the 0.1–2.0 THz frequency range, using time domain spectroscopy (TDS) [20]. A commercial equipment, TPS Spectra 3000 (Teraview, Ltd., Cambridge, UK), was used to this end. During the measurement, two spectrograms were obtained: a reference spectrogram, to take into account the influence of the setup; and a spectrogram of the investigated material using a probe of constant thickness. The transmission type measurement, executed in the time domain, provided the phase difference of the radiation passing through the sample φ , and the reference setup φ_r ; then, the refractive index as a function of frequency, ν , was calculated in terms of the sample thickness, d , as [21–23]

$$n(\nu) = 1 + c(\varphi_s(\nu) - \varphi_r(\nu))/(2\pi\nu d). \quad (1)$$

The results are presented in Fig. 1. Prototypes of diffractive lenses were constructed in these materials to select the one that presented the highest fidelity compared to the original design PA 6 with a refractive index $n = 1.59$, and absorption coefficient 3.09 cm^{-1} at 0.625 THz was selected for the realization of the lenses. Unless this material was previously characterized by

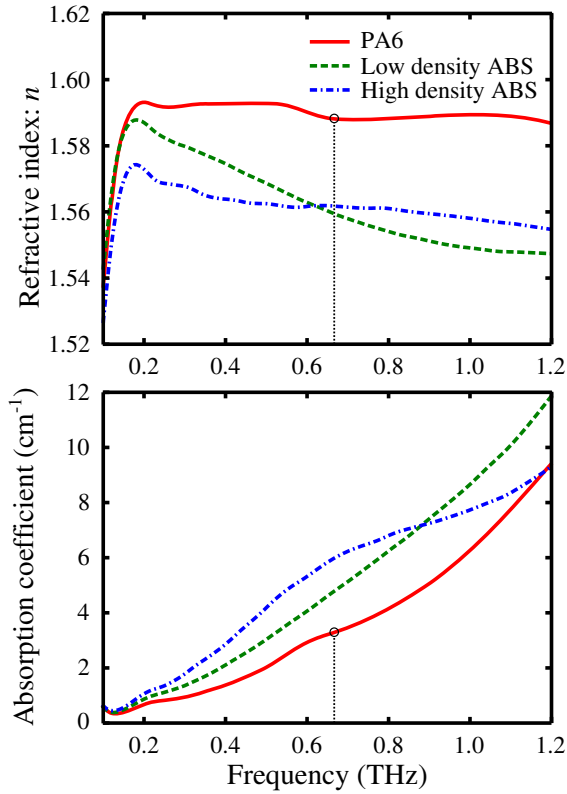


Fig. 1. Refractive index of various materials obtained in the TDS system.

using a THz time-domain spectrometry in the frequency range 2–15 THz [24], to the best of our knowledge, to date PA6 has not been measured for lower frequencies or used to construct diffractive lenses.

In designing THz diffractive lenses, we followed the procedure described in detail in [18] and [19]. In this case, the fractal zone plate was based on a triadic Cantor set for stage 2, and the Fibonacci zone plate was based on the Fibonacci sequence of order 5. Figure 2 shows the experimental models which were designed using a browser-based CAD software (Tinkercad.com) and constructed with a 0.3 mm spatial resolution by an online 3D printing service (i.materialise, Leuven, Belgium), which were made from a polyamide granular powder by selective laser sintering technique.

The diameter of the Fresnel and fractal lenses was 4.62 cm, having the main focal distance (first diffraction order) $f = 12.35$ cm. The bifocal Fibonacci lens diameter was 4.94 mm, with focal distances $f_1 = 12.9$ cm and $f_2 = 20.0$ cm. All lenses had the same base layer thickness, 1 mm, and groove height, 0.4 mm; which has been calculated to provide alternating zones with a 0 and π phase delay for the design frequency, 625 GHz.

Using the nonparaxial scalar diffraction theory, the axial irradiance provided by these lenses of a given radius a was numerically evaluated as

$$I(z) = \left| \int_0^1 \exp[i\pi\phi(\zeta)] \cdot \frac{\exp\left[\frac{2\pi ia}{\lambda} \sqrt{\zeta + \left(\frac{z}{a}\right)^2}\right]}{\sqrt{\zeta + \left(\frac{z}{a}\right)^2}} d\zeta \right|^2, \quad (2)$$

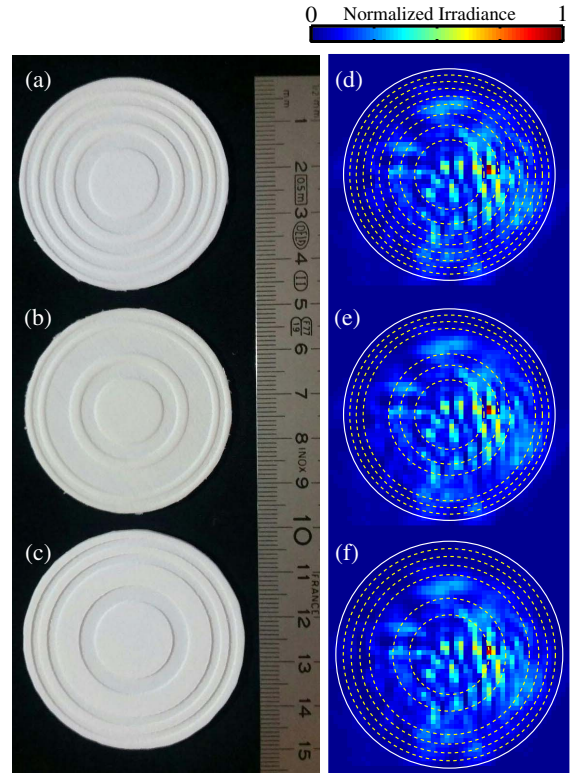


Fig. 2. Experimental (a) Fresnel, (b) fractal, and (c) Fibonacci models of 3D printed THz diffractive lenses made PA6. Map of the THz irradiance measured at the plane of the lens in the experimental setup represented in Fig. 3 (dotted lines represent the phase transitions) for (d) Fresnel, (e) fractal, and (f) Fibonacci lenses.

where λ is the wavelength, z is the propagated distance, and $\phi(\zeta)$ defines the phase distribution of the studied lens represented in terms of the square normalized radial coordinate, $\zeta = (r/a)^2$. The phase function $\phi(\zeta)$ for Fresnel lenses can be written as a Ronchi-type periodic binary function with period p :

$$\phi(\zeta) = \phi_F(\zeta, p) = \text{rect}[\zeta - 0.5] \cdot \text{rect}\left[\frac{\text{mod}[\zeta + 0.5p - 1, p]}{p}\right], \quad (3)$$

where $p = 2/9$ for the Fresnel lens shown in Fig. 2(a), and the function $\text{mod}[x, y]$ gives the remainder on division of x by y . The corresponding phase function $\phi(\zeta)$ for triadic Cantor lenses developed up to a certain growing stage S can be written as the above periodic function as

$$\phi(\zeta) = \phi_{\text{Frac}}(\zeta, S) = \prod_{i=0}^S \phi_F(\zeta, 2/3^i), \quad (4)$$

being $S = 2$ for the fractal lens shown in Fig. 2(b). In the case of a Fibonacci lens of order S , the phase function $\phi(\zeta)$ is given by

$$\phi(\zeta) = \phi_{\text{Fibonacci}}(\zeta, S) = \sum_{i=0}^{F_S} \text{rect}[\zeta F_{S+1} + 0.5 + [i\phi]], \quad (5)$$

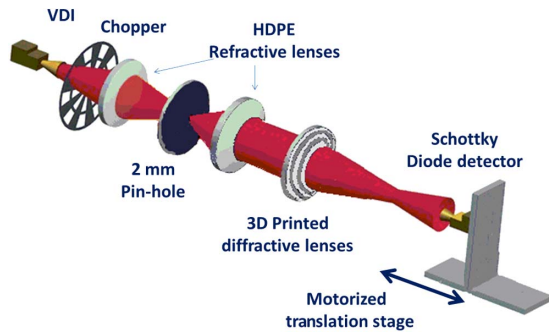


Fig. 3. Scheme of the optical setup used for axial PSF measurements.

where F_j is the Fibonacci number of order j , φ is the golden ratio [19], and $[x]$ denotes the largest integer less than or equal to x . Figure 2(c) shows a Fibonacci lens of order $S = 5$.

The experimental setup for the optical characterization of the lenses is shown in Fig. 3. The axial point spread function (PSF) was measured with a 625 GHz beam provided by a VDI frequency multiplier (Virginia Diodes, Inc., Charlottesville, VA, USA). The emitter was equipped with a horn antenna which produced a divergent beam, which was focused by a high-density polyethylene (HDPE) refractive lens into a pin-hole (2 mm diameter). Next, the beam was collimated by a second HDPE lens and directed to the investigated diffractive lens. Figures 2(d)–2(f) show the local irradiance of the electromagnetic field at the plane of the lenses. The local maxima and minima of irradiance were caused by interferences during beam propagation. Besides, the main spots are not perfectly centered because, despite the experimental setup being carefully configured to maintain the center of the beam on the optical axis, a small misalignment still remained. The focal volume was axially scanned with a Schottky diode (equipped with a horn antenna) mounted on a motorized stage. Due to its finite size, the detector integrates the irradiance in an area of $2.5 \text{ mm} \times 2.5 \text{ mm}$ around the optical axis.

Experimental results for the axial PSF are represented in Fig. 4 (dotted red points), together with the numerical results (continuous green lines) computed using Eqs. (2)–(5). As can be seen, the fractal binary lens has an extended depth of focus compared with a conventional Fresnel zone plate, while a Fibonacci lens splits the main focus, providing a pair of foci satisfying $f_1/f_2 \approx \varphi$. Although the experimental results are affected by the finite size of the detector and by the inhomogeneity of the THz beam [see Figs. 2(d)–2(f)], a very good agreement between theory and experiment can be observed.

Summarizing, we have demonstrated the feasibility of realizing high-quality THz diffractive lenses with 3D printing technology. The focusing properties of nonconventional lenses named fractal and Fibonacci zone plates were tested using 0.625 THz beam for the first time, to the best of our knowledge. Using nonparaxial scalar diffraction theory, we have shown numerically the special performance of such lenses which were confirmed experimentally using a simple experimental THz PSF setup. We found that T-ray fractal zone binary lenses have an extended depth of focus, compared with the Fresnel zone plate, which opens the possibility to fabricate optics with low chromatic aberration for wideband THz applications. Concerning diffractive THz optics with extended

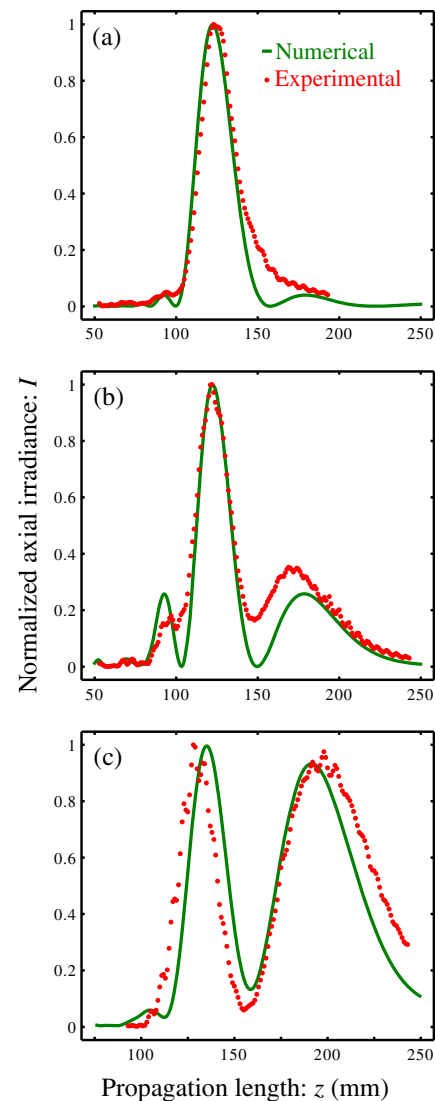


Fig. 4. Numerical simulation, continuous (green) lines and experimental results (dotted) red lines provided by the 3D printed THz lenses of Fig. 2: (a) Fresnel, (b) fractal, and (c) Fibonacci.

depth of focus, Agafonov *et al.* [25] recently presented interesting results of a silicon binary diffractive optical element focusing a THz laser Gaussian beam into a paraxial segment. On the other hand, a bifocal Fibonacci THz lens has been also constructed, which has potential applications in THz quality control systems or THz medical diagnosis and therapy [26]. Moreover, with the advance of the 3D technology, better resolutions will allow the construction of lenses with multilevel (even kinoform) diffractive structures with improved diffraction efficiency.

Although, for our investigations, we have chosen Fresnel, fractal, and Fibonacci lenses of fixed focal lengths, the versatile 3D printing technology can be applied to construct lenses with different focal lengths and geometries (multiorder, elliptical, conical, etc.), and even array of lenses with any spatial distribution. Moreover, the diffraction efficiency can be increased with the number of phase levels. Work is in progress in these directions.

Funding. Ministerio de Economía y Competitividad (MINECO) (FIS2011-23175); Generalitat Valenciana (PROMETEOII/2014/072); National Center for Research and Development in Poland (LIDER/020/319/L-5/13/NCBR/2014).

Acknowledgment. The authors thank A. Hermida for his help in the 3D printing of the prototypes.

REFERENCES

1. R. Wilk, N. Vieweg, O. Kopschinski, and M. Koch, *Opt. Express* **17**, 7377 (2009).
2. V. Astley, J. Scheiman, R. Mendis, and D. M. Mittleman, *Opt. Lett.* **35**, 553 (2010).
3. B. Scherger, M. Scheller, N. Vieweg, S. T. Cundiff, and M. Koch, *Opt. Express* **19**, 24884 (2011).
4. B. Scherger, C. Jördens, and M. Koch, *Opt. Express* **19**, 4528 (2011).
5. B. Scherger, M. Scheller, C. Jansen, M. Koch, and K. Wiesauer, *Appl. Opt.* **50**, 2256 (2011).
6. A. Podzorov and G. Gallot, *Appl. Opt.* **47**, 3254 (2008).
7. S. Wang, T. Yuan, E. Walsby, R. J. Blaikie, S. M. Durbin, D. R. S. Cumming, J. Xu, and X.-C. Zhang, *Opt. Lett.* **27**, 1183 (2002).
8. Y. Yu and W. Dou, *Opt. Express* **17**, 888 (2009).
9. P. F. Goldsmith, in *Third International Symposium on Space Terahertz Technology* (1992), pp. 345–361.
10. J. C. Wiltse, *Defense and Security*, R. J. Hwu, D. L. Woolard, and M. J. Rosker, eds. (International Society for Optics and Photonics, 2005), pp. 167–179.
11. A. Siemion, A. Siemion, M. Makowski, J. Suszek, J. Bomba, A. Czerwinski, F. Garet, J.-L. Coutaz, and M. Sypek, *Opt. Lett.* **37**, 4320 (2012).
12. A. N. Agafonov, B. O. Volodkin, A. K. Kaveev, B. A. Knyazev, G. I. Kropotov, V. S. Pavel'ev, V. A. Soifer, K. N. Tukmakov, E. V. Tsygankova, and Y. Y. Choporova, *Optoelectron. Instrum. Data Process.* **49**, 189 (2013).
13. E. D. Walsby, S. Wang, J. Xu, T. Yuan, R. Blaikie, S. M. Durbin, X.-C. Zhang, and D. R. S. Cumming, *J. Vac. Sci. Technol. B* **20**, 2780 (2002).
14. M. S. Komlenok, B. O. Volodkin, B. A. Knyazev, V. V. Kononenko, T. V. Kononenko, V. I. Konov, V. S. Pavelyev, V. A. Soifer, K. N. Tukmakov, and Y. Y. Choporova, *Quantum Electron.* **45**, 933 (2015).
15. M. F. Busch, M. Weidenbach, M. Fey, F. Schäfer, T. Probst, and M. Koch, *J. Infrared Millim. Terahertz Waves* **35**, 993 (2014).
16. A. D. Squires, E. Constable, and R. A. Lewis, in *39th International Conference on Infrared, Millimeter, and Terahertz Waves (IRMMW-THz)* (IEEE, 2014), pp. 1–2.
17. J. Suszek, A. Siemion, M. S. Bieda, N. Blocki, D. Coquillat, G. Cywinski, E. Czerwinska, M. Doch, A. Kowalczyk, N. Palka, A. Sobczyk, P. Zagrajek, M. Zaremba, A. Kolodziejczyk, W. Knap, and M. Sypek, *IEEE Trans. Terahertz Sci. Technol.* **5**, 314 (2015).
18. G. Saavedra, W. D. Furlan, and J. A. Monsoriu, *Opt. Lett.* **28**, 971 (2003).
19. J. A. Monsoriu, A. Calatayud, L. Remón, W. D. Furlan, G. Saavedra, and P. Andrés, *IEEE Photon. J.* **5**, 3400106 (2013).
20. Y.-S. Lee, *Principles of Terahertz Science and Technology* (Springer, 2009).
21. P. Y. Han and X.-C. Zhang, *Meas. Sci. Technol.* **12**, 1747 (2001).
22. M. Hangyo, T. Nagashima, and S. Nashima, *Meas. Sci. Technol.* **13**, 1727 (2002).
23. M. Naftaly and R. E. Miles, *Proc. IEEE* **95**, 1658 (2007).
24. F. D'Angelo, Z. Mics, M. Bonn, and D. Turchinovich, *Opt. Express* **22**, 12475 (2014).
25. A. N. Agafonov, B. O. Volodkin, D. G. Kachalov, B. A. Knyazev, G. I. Kropotov, K. N. Tukmakov, V. S. Pavelyev, D. I. Tsypishka, Y. Y. Choporova, and A. K. Kaveev, *J. Mod. Opt.* **1**, 1 (2015).
26. W.-Q. Liu, Y.-F. Lu, G.-H. Jiao, X.-F. Chen, J.-Y. Li, S.-H. Chen, Y.-M. Dong, and J.-C. Lv, *Opt. Commun.* **359**, 344 (2016).